CHEMISTRY
A European Journal

Supporting Information

Ag^{I}-Induced Switching of DNA Binding Modes via Formation of a Supramolecular Metallacycle

Shibaji Basak[+],[a] J. Christian Léon[+],[b] Annaleizle Ferranco,[a] Renu Sharma,[a] Marian Hebenbrock,[b] Alan Lough,[c] Jens Müller,*[b] and Heinz-Bernhard Kraatz*[a, c]

chem_201800440_sm_miscellaneous_information.pdf

Contents

Experimental Section

Materials and reagents.

HCl.H_2N-His(Trt)COOMe was purchased from Aapptec. Whereas, 1,4,5,8-Naphthalenetetracarboxylic dianhydride (NDA), Trifluoroacetic acid (TFA), Triethylsilane and $AgBF_4$ were purchased from Sigma Aldrich. Sulfuric acid (98%), sodium hydroxide, silver nitrate and potassium nitrate were obtained from Caledon (Georgetown, ON). Hydrogen peroxide (30%), 3-(*N*-morpholino)propanesulfonic acid, agar, sodium perchlorate, potassium ferrocyanide and potassium ferricyanide were bought from Sigma-Aldrich (Oakville, ON). Alumina powders (0.3 μm and 0.05 μm, respectively) were obtained from Allied High Tech Product (Compton, CA). Potassium ferrocyanide and sodium perchlorate was purchased from Sigma-Aldrich (Oakville, ON). All aqueous solutions were prepared using deionized water (Millipore Milli-Q; 18 MΩcm resistivity). The reagents were used as received. Milli-Q water was used throughout this study for all purposes including electrochemistry, sample solutions and rinsing.

Nuclear magnetic resonance (NMR): All liquid-phase NMR studies were carried out on a Agilent DD2 500 MHz, 300 K using MeOD maintaining the concentration 10 mM. Chemical shifts (δ) were reported in ppm for all 1D-H NMR. Data processed in MestReNova software.

Mass spectroscopy: All experiments were performed on Agilent Technologies 6530 Accurate-Mass Q-TOF LC/MS spectrometer.

Circular Dichroism (CD) spectra. CD experiments were recorded with a JASCO J-810 spectrometer using a 1 mm path-length cell. All CD experiments were performed at 25 °C.

ITC Study: ITC measurements were performed with TA instruments Nano ITC Low Volume instrument (Waters Corp., Milford, MA, USA) with cell volume of 250 μL using ITC Run version 2.1.7.0 Firmware version 1.31 (TA instruments, Waters Corp., Milford, MA, USA) as software. The reference cell was filled with deionized water and all the solutions were degassed for 10 min prior to measurements. The titrations were performed automatically by adding 2.5 μL aliquots of prepared concentrated stock solution of 1 mM $AgClO_4$ solution in buffer (150 mM $NaClO_4$, 5 mM MOPS, pH 6.8) into the sample cell containing 250 μL of 10 μM of DNA and **L1** solution with continuous stirring of 200 rpm. All the solutions were made in the same buffer solution. Measurements were performed in duplicate.

Fourier Transform Infrared Spectroscopy (FTIR). Sample was allowed to dry in air and FTIR spectra were recorded using a Bruker ALPHA FTIR spectrometer equipped with a diamond ATR.

Spectroscopy: UV spectra were obtained using solutions containing 0.3 μM CT-DNA, 1 mM $NaClO_4$, and 5 mM MOPS at pH 6.8. UV spectra were recorded on a CARY BIO 100 spectrophotometer.

Synthesis Procedure

NDI-(His(Trt)COOMe)$_2$: 670 mg (1.5 mmol) of HCl.H_2N-His(Trt)COOMe was taken in water (20 ml) and covered with ethyl acetate (about 50 ml) and basified with a solution of $NaHCO_3$. The aqueous phase was extracted with ethyl acetate and this operation was done repeatedly. The ethyl acetate extracts were pooled, washed with brine and dried over anhydrous Na_2SO_4 and evaporated in *vacuum*. A white material was obtained. To this white material, NDA (130 mg, 0.5 mmol) was added and placed in a round-bottomed flask along with dry DMF (15 ml) and the reaction mixture was stirred for 12 h at 140 °C under N_2 atmosphere. The heating was stopped and the solution was allowed to cool to room temperature and 30 mL dichloromethane was added. The organic layer was washed with 1N HCl (3 × 30 ml), brine (3 × 30 ml) and dried over anhydrous Na_2SO_4 and evaporated in *vacuum.* The product was further purified by column chromatography by using silica gel as stationary phase and MeOH in $CHCl_3$ as eluent.

Yield: 210 mg (0.2 mmol, 40 %).

^{1}H NMR (500 MHz, $CDCl_3$) δ 8.67 (4H, NDI, s), 7.28-6.88 (30H, aromatic Hs, m), 6.56 (2H, imidazole ring, s), 6.05-6.02 (2H, $^{\alpha}$H, t, J = 7.5), 3.78 (6H, OCH_3, s), 3.58-3.55 (4H, $^{\beta}$Hs, m). 13C NMR (126 MHz, $CDCl_3$) δ 162.34, 130.97, 129.55, 127.86, 127.78, 126.82, 126.41, 77.24, 76.99, 76.74, 54.06, 52.60, 29.46, 27.10. Anal. Calcd. : $C_{66}H_{50}N_6O_8$ (1054.3690): MS (ESI) m/z 1055.3777 $[M+H]^+$.

NDI-(His-COOMe)$_2$ (L1): 210 mg (0.2 mmol) of NDI-(His(Trt)COOMe)$_2$ was dissolved in DCM and 26 mg (0.22 mmol) of triethylsilane was added. The reaction mixture was stirred under N_2 atmosphere. After 15 minute, 1 mL of TFA was added to the reaction mixture. After 1hr, the TFA was removed under vacuum. The reaction product was diluted with water and washed with diethyl ether. The clear water part then neutralized by NH_4OH solution and lyophilised. A brown solid obtained which gives brown coloured crystals at room temperature from water suitable for crystallography.

Yield: 90 mg (0.16 mmol, 80 %).

^{1}H NMR (500 MHz, MeOD) δ 8.70 (4H, NDI, s), 7.41 (2H, imidazole ring, s), 6.76 (2H, imidazole ring, s), 6.03-6.00 (2H, $^{\alpha}$H, m), 3.77 (6H, OCH_3, s), 3.62-3.48 (4H, $^{\beta}$Hs, m); ^{13}C NMR (126 MHz, MeOD) δ 171.37, 163.72, 136.24, 132.22, 128.08, 127.73, 55.12, 53.12. FT-IR (cm^{-1}), 769, 1254, 1336, 1451, 1453, 1582, 1664, 1703, 1745, 2600-3500 (br). Anal. Calcd.: $C_{28}H_{22}N_6O_8$ (570.1499): MS (ESI) m/z 571.1576 $[M+H]^+$.

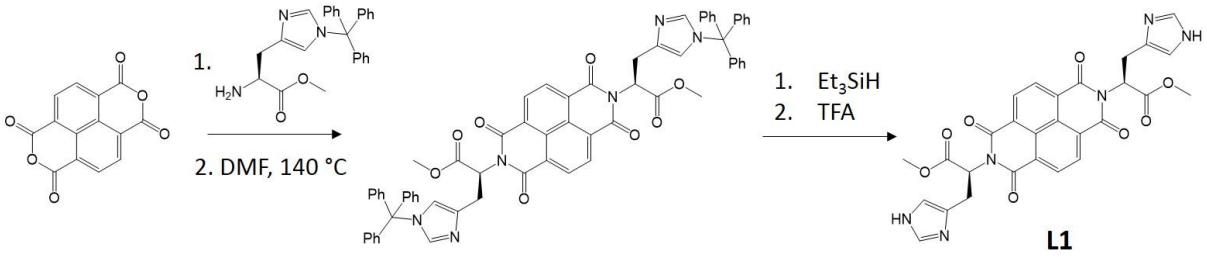

Scheme S1: Synthesis of the ligand **L1**.

The **synthesis of the nucleotides** has been reported elsewhere.[1] A duplex consisting of ODN 1/2 was used for studies in solution while a duplex consisting of ODN 3/2 was used to form DNA films on a gold surface.

ODN 1 5 '-d(TTT GTT TGT TTG TTT GTT TTT TTT TT)-3‘

ODN 2 3'-d(AAA CAA ACA AAC AAA CAA AAA AAA AA)-5‘

ODN 3 HO-$(CH_2)_3$-S-S-$(CH_2)_3$-5 '-d(TTT GTT TGT TTG TTT GTT TTT TTT TT)-3‘

Calf thymus DNA (fibrious) was purchased by Sigma Aldrich.

Electrochemistry

To **fabricate the electrodes** used in this work**,** CHI101 gold disc electrodes (with a radius of 1 mm) were treated with “Piranha” solution (98% H_2SO_4 / 30% H_2O_2 : 3/1 (v/v)). After polishing in alumina slurries (1 µm, 0.3 µm and 0.05 µm) for 3 minutes, the electrodes were ultra sonicated in Milli-Q H_2O and ethanol. The Electrodes were cleaned electrochemically in KOH (0.5 M, -2 to 0 V at 0.5 Vs^{-1}) and H_2SO_4 (0.5 M, 0 to 1.5 V at 0.5 Vs^{-1}) for at least 300 cycles each until scans were reproducible. To immobilize the DNA on the gold surface, the electrode was stored in DNA solution (25 µM dsDNA, 150 mM $NaClO_4$, 5 mM MOPS at pH 6.8) for 3 days. To prevent the $[Fe(CN)_6]^{3-/4-}$ redox probe from interacting with the gold surface the film holes were blocked by treatment with 6-mercaptohexan-1-ol solution (1 mM MCH, 150 mM $NaClO_4$, 5 mM MOPS at pH 6.8) for 2 h. The electrode was treated with Ag^{I}-, **L1**- or **C2** solution (10 µM analyte, 150 mM $NaClO_4$, 5 mM MOPS at pH 6.8). After each step, the electrode was carefully washed with buffer (150 mM $NaClO_4$, 5 mM MOPS at pH 6.8).

The **electrochemical measurements** were performed in a Faraday cage. EIS measurements were carried out on a CHI-6059E potentiostat (CH instruments, Austin, TX) by using a cell with three electrodes: a DNA modified gold electrode (working electrode), a platinum wire (counter electrode)

and a Ag/AgCl (3.0 M KCl; reference electrode). Diffusion of chloride into the electrolyte solution and following interaction with Ag^{I} was prevented by a salt bridge containing agar gel in 1 M KNO_3 which was inserted between the $[Fe(CN)_6]^{3-/4-}$ solution and the reference KCl solution. An aqueous solution of 2 mM $K_4[Fe(CN)_6]$/2 mM $K_3[Fe(CN)_6]$, 150 mM $NaClO_4$ (supporting electrolyte) and 5 mM 3-(*N*-Morpholino)propanesulfonic acid (MOPS, pH 6.8) was used as electrolyte and redox probe. All EIS measurements were performed with open circuit potentials and with a frequency range from 100 000 to 0.1 Hz with an amplitude of 5 mV. The software ZSimpWin 2.0 was used to perform simulations on the EIS results by using a modified Randles' equivalent circuit (Scheme S2). R_S (solution resistance) accounts for the resistance between the gold surface and the platinum wire.[2 ENREF 3] The solution conditions (2 mM mM $[Fe(CN)_6]^{4-}$, 5 mM MOPS, 150 mM $NaClO_4$) are kept constant to prevent variations in R_S. The capacitance of the DNA film is shown as C_M. The properties of MCH-diluted films are represented by the constant phase element (CPE) and R_X.[3 ENREF 4] Finally, the resistance of the DNA films towards charge transfer between the gold surface and the redox probe is shown as R_{CT}.

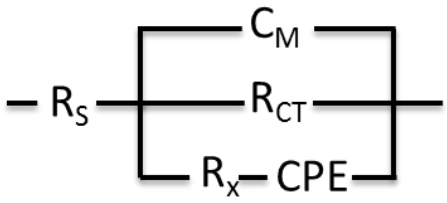

Scheme S2: Modified Randles' equivalent circuit used to analyze the EIS results.

NMR-Spectra

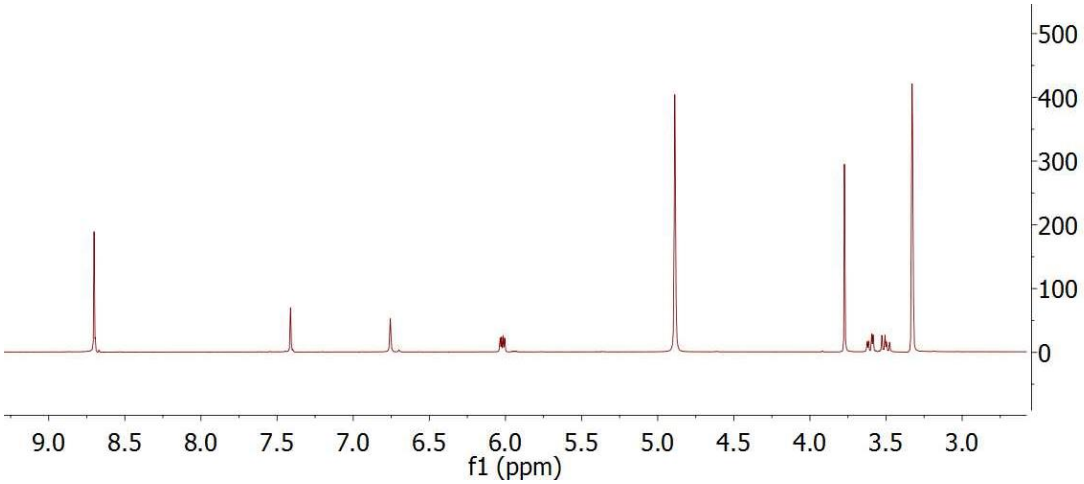

Figure S1. ^{1}H NMR spectrum of **L1** in MeOD.

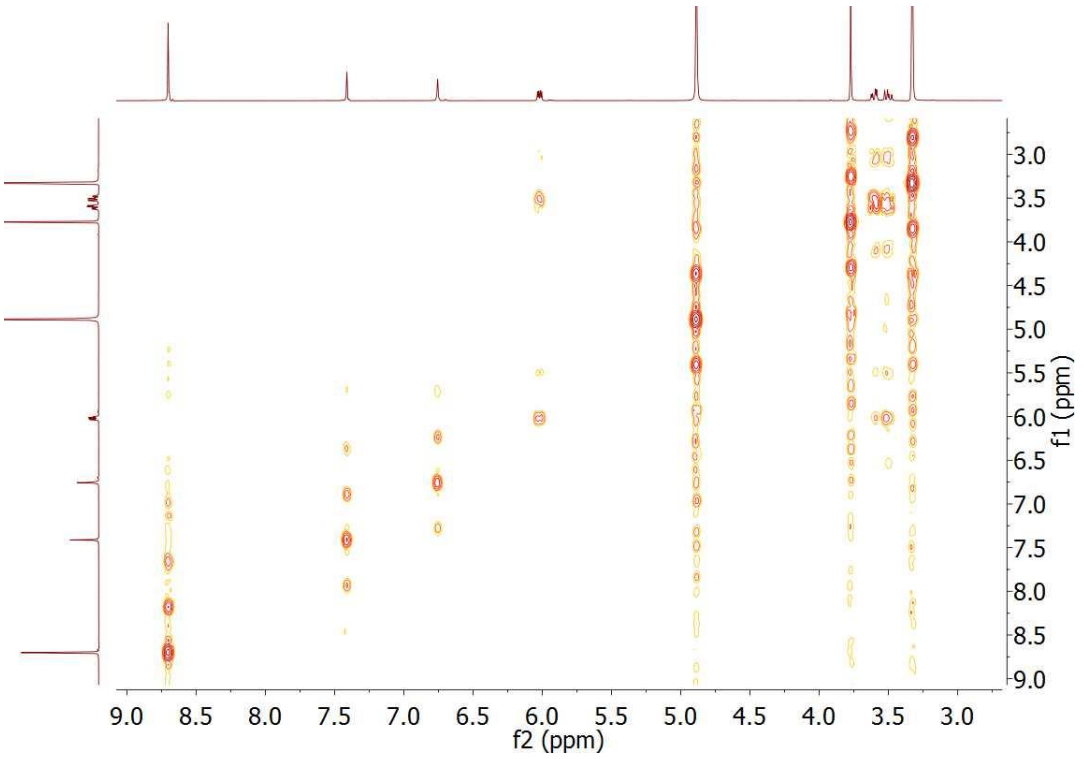

Figure S2. ^{1}H-^{1}H COSY NMR of **L1** in MeOD.

Crystallographic Data

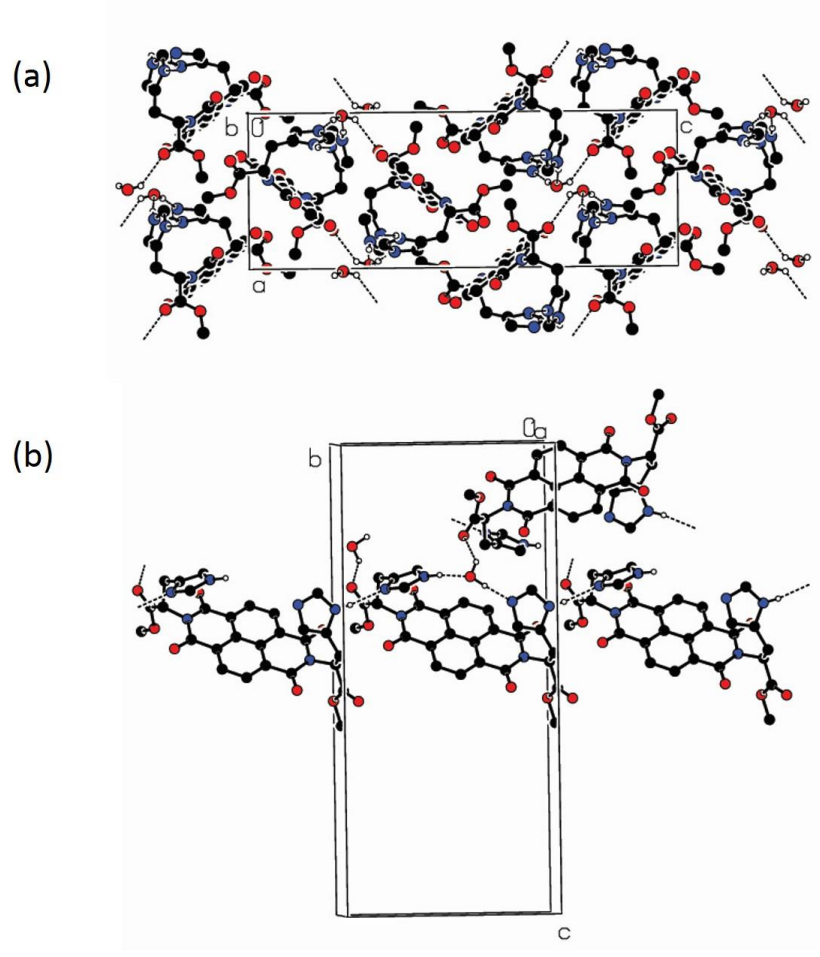

Figure S3. Crystal packing of **L1**. One nitrogen atom of each imidazole groups of the same ligand molecule is connected to a water molecule by intramolecular hydrogen bond bridge. The so formed bridged hydrogen bonds formed a bent structure of the ligand **L1**. Each water molecule is connected

to a carbonyl functionality of the ester group of a neighbouring ligand molecule through intermolecular hydrogen bonding. The other nitrogen atom of each imidazole ring is connected to a nitrogen atom of imidazole group of neighbouring ligand molecule through intermolecular hydrogen bonding. The dotted line represents the hydrogen bond.

(a)

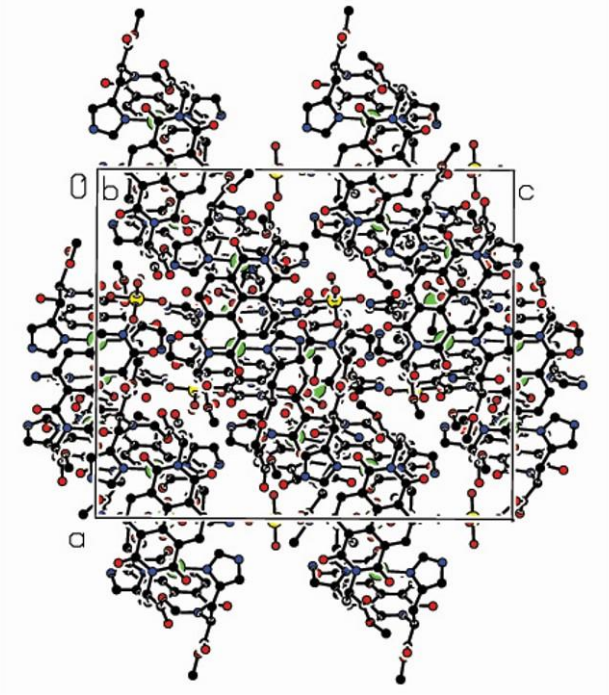

(b)

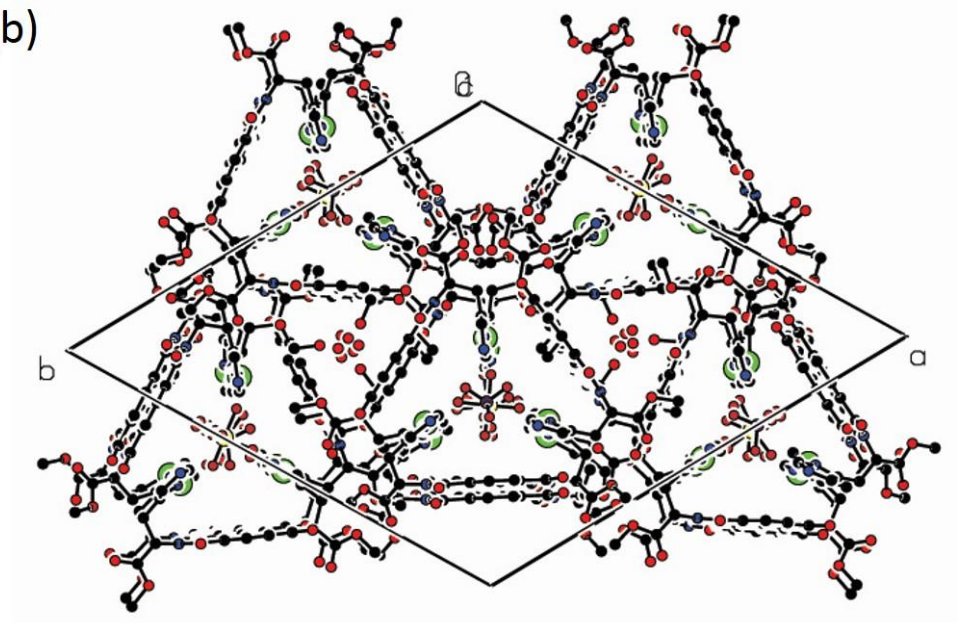

Figure S4. Crystal packing of **C2** along b-axis **(a)** and c-axis **(b)**. Hydrogen atoms are omitted for clarity.

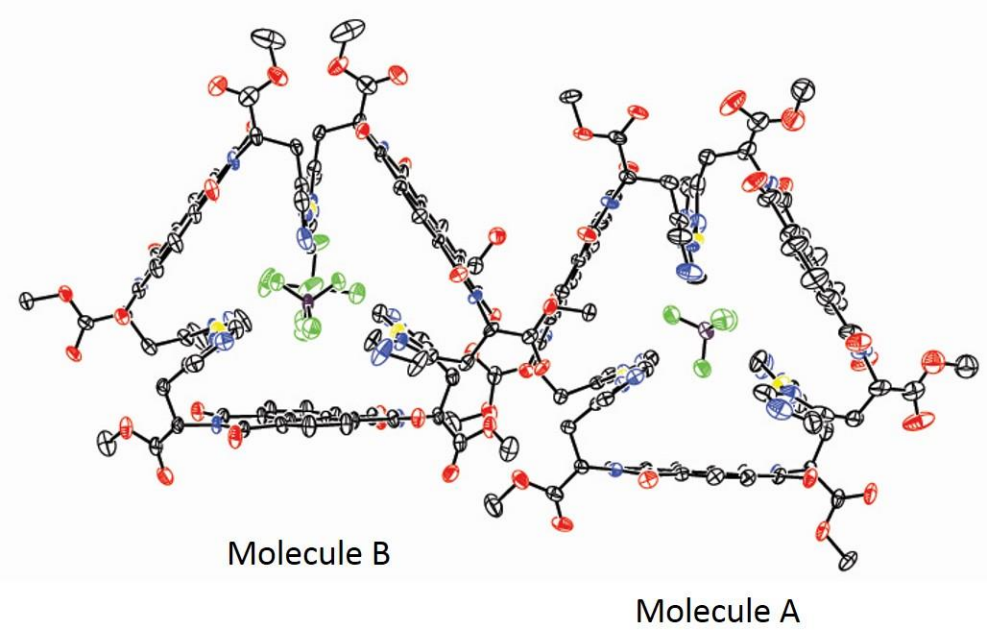

Figure S5. Molecular structures of the macrocycle **C2** (hydrogen atoms are omitted for clarity). The molecular structure showed two crystallographically independent macrocycles (labelled as Molecule A and Molecule B) formed which are composed of six ligands and six Ag^{I} ions coordinated through the nitrogen atoms of the histidine imidazole rings. The BF_4^- counter anions were placed perfectly inside the centre of each triangular macrocycle. To our surprise we found one SiF_6^{2-} anion situated outside the middle of one half molecule and stabilizing the macrocyclic crystal packing. However, none of the starting material contain any SiF_6^{2-} ions in excess. The SiF_6^{2-} ions presumably generates in the system by the reaction of HF with the inner wall of the glass tube. The hydrolysis of the BF_4^- ions to HF is well reported in aqueous media.[4a] Thus, so formed HF molecules readily react with inner wall of the glass tube and consequently yields SiF_6^{2-} ions as a result of glass etching.[4b]

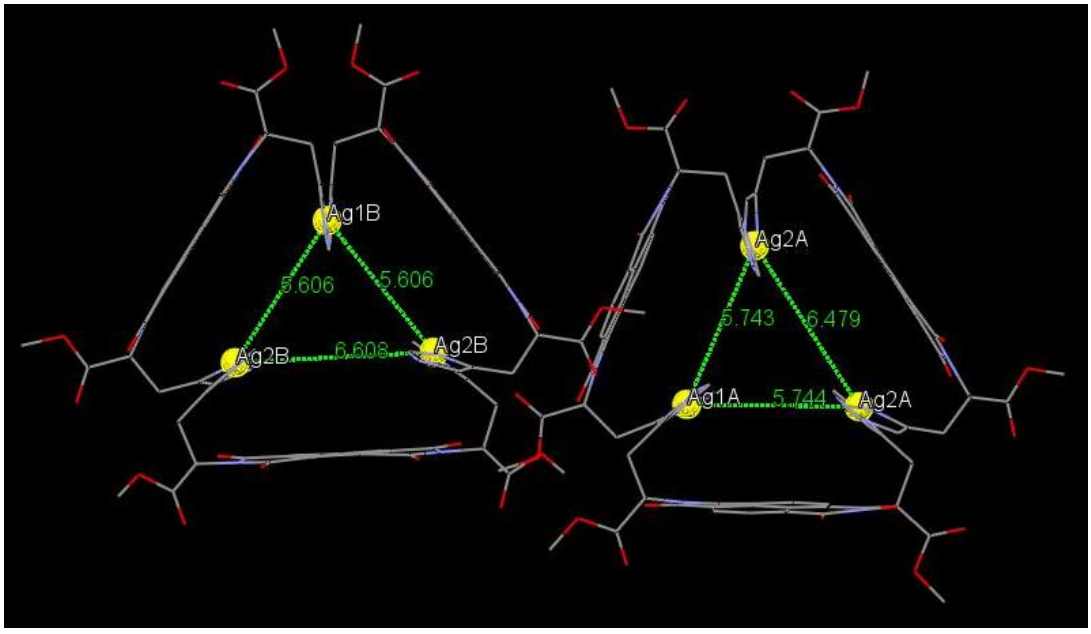

Figure S6. Molecular structures of the macro cycle **C2** in wireframe model (hydrogen atoms, solvent molecules and counter anions are omitted for clarity). The Ag-Ag (displayed in ball and stick) distances are identical for two Ag centres (Ag1A….Ag2A, 5.60 Å; Ag1B….Ag2B, 5.74 Å) while the third one is different from the former (Ag2A….Ag2A, 6.60 Å; Ag2B….Ag2B, 6.47 Å) in each macrocycle (Ag, yellow; C, gray; N, purple; O, red).

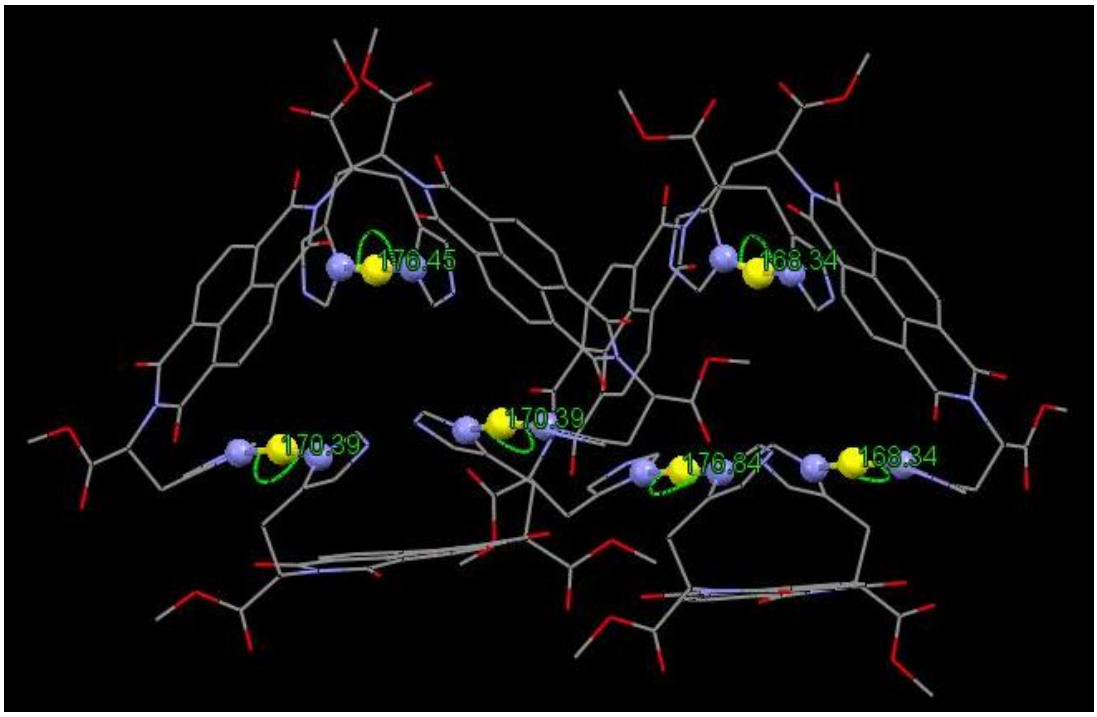

Figure S7. Molecular structures of the macrocycle **C2** in wireframe model (hydrogen atoms, solvent molecules and counter anions are omitted for clarity) shows the N-Ag-N bond angles. The N-Ag-N (displayed in ball and stick) bond angle values for N(4A)#1-Ag(1A)-N(4A), 176.9(3); N(7A)-Ag(2A)-N(6A), 168.4(4)) and (N(4B)-Ag(1B)-N(4B)#2, 176.5(4); N(7B)-Ag(2B)-N(6B), 170.4(3). Ag, yellow; C, gray; N, purple; O, red.

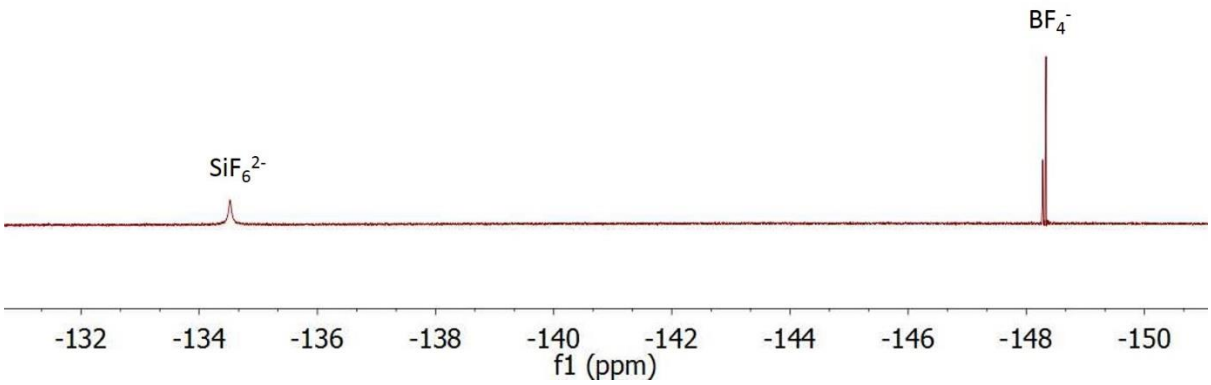

Figure S8. ^{19}F NMR spectrum of the macrocycle in DMSO-D_6 display the signals for BF_4^- ion at -148.33 and SiF_6^{2-} ion at -134.52. The small peak at -148.28 could be attributed to the BF_4^- ions which are not inside the macrocycles in solution.[5]

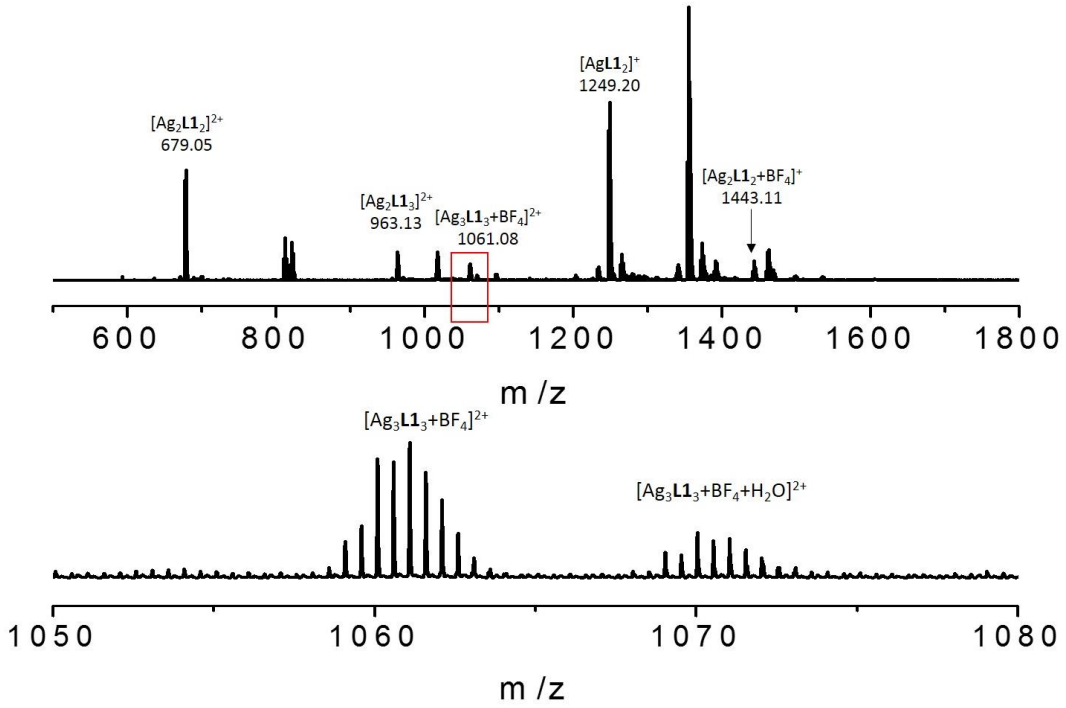

Figure S9. The ESI-MS spectrum showed the peaks for the macrocycle **C2** and dimeric fragment of **C2**. The peak for $[Ag^{I}_{3}\mathbf{L1}_{3}]^{3+}$ and $[Ag^{I}_{2}\mathbf{L1}_{2}]^{2+}$ at m/z = 679.0548 are merged together and hard to distinguish. However, MS-data showed peak for $[Ag^{I}_{3}\mathbf{L1}_{3}.BF_4]^{2+}$ at m/z = 1061.5848 and a peak for $[Ag^{I}_{3}\mathbf{L1}_{3}.BF_4.H_2O]^{2+}$ at m/z = 1070.5286 clearly indicate the presence of those species in solution. The ESI-Ms analysis was performed by dissolving single crystals of **C2** in water.

Characterization of the binding modes

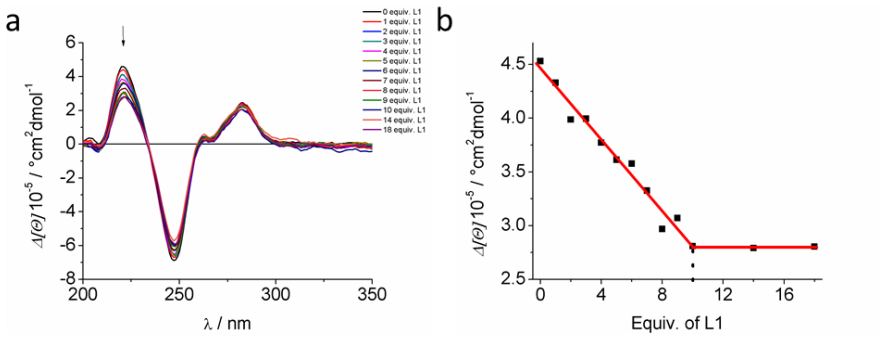

Figure S10. a) CD spectra of a DNA duplex titrated with **L1**. No major conformational changes were observed. Small decrease in signal intensity at 220 nm can be detected, with no further decrease

after the addition of ten equiv. of **L1**. b) Signal intensity plotted against the equiv. of **L1** added to the solution. Experimental conditions: 1 µM duplex, 150 mM $NaClO_4$ and 5 mM MOPS (pH 6.8).

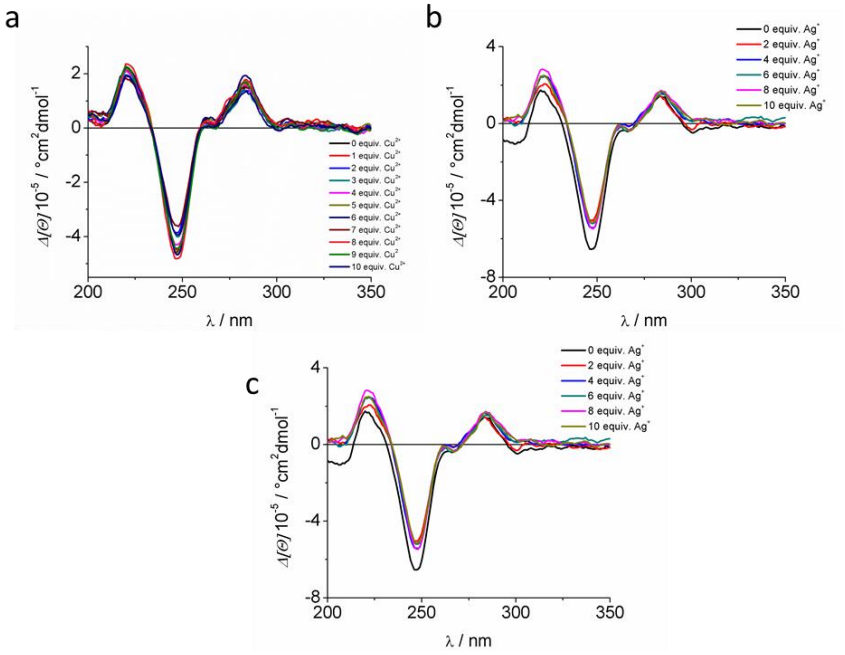

Figure S11. CD spectra of a) a DNA duplex with ten **L1** molecules intercalated and then titrated with various amounts of Cu^{II} to block the histidine binding sites. In contrast to the same experiment with AgI, no major changes can be observed. b) a duplex with ten L1 molecules intercalated, ten Cu^{II} added and then titrated with Ag^{I}. Again, no changes were observed. c) Control experiment to exclude interactions of DNA with Ag^{I}. A DNA duplex titrated with Ag^{I}. Experimental conditions: 1 µM duplex, 150 mM $NaClO_4$ and 5 mM MOPS (pH 6.8).

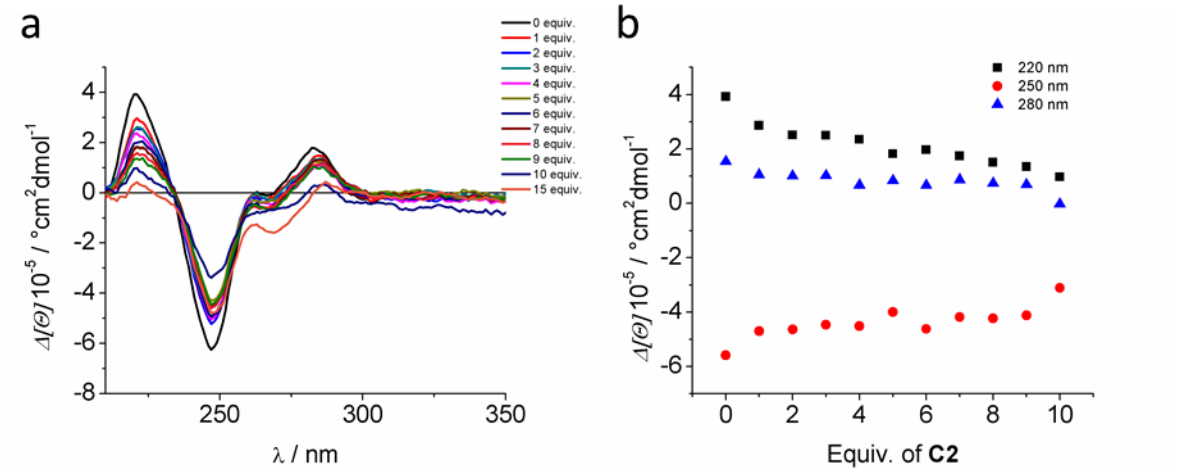

Figure S12. CD spectra of a) a DNA duplex titrated with **C2** b) Intensity of the CD features at 280 (▲), 250 (●) and 220 (■) nm. The intensity of the characteristic CD features of DNA decrease with increasing amount of **C2** present in solution. Experimental conditions: 1 µM duplex, 150 mM $NaClO_4$ and 5 mM MOPS (pH 6.8).

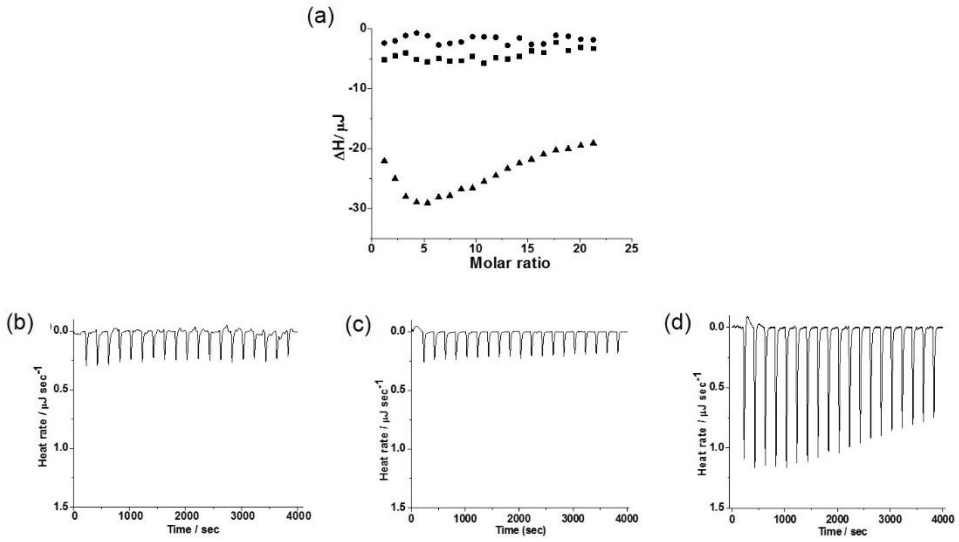

Figure S13. a) Plot of the integrated heat features against the molar ratio for **L1** in MOPS buffer (●), **L1** vs DNA (■) and mixture of Ag^{I} and **L1** vs DNA (▲). ITC raw data for (b) **L1** in MOPS buffer, (c) **L1** vs DNA and (d) mixture of **L1** and Ag^{I} vs DNA. In all titrations, the former is taken in syringe and other in the cell while the total concentrations of solutions taken in syringe and cell are 1 mM and 10 µM respectively.

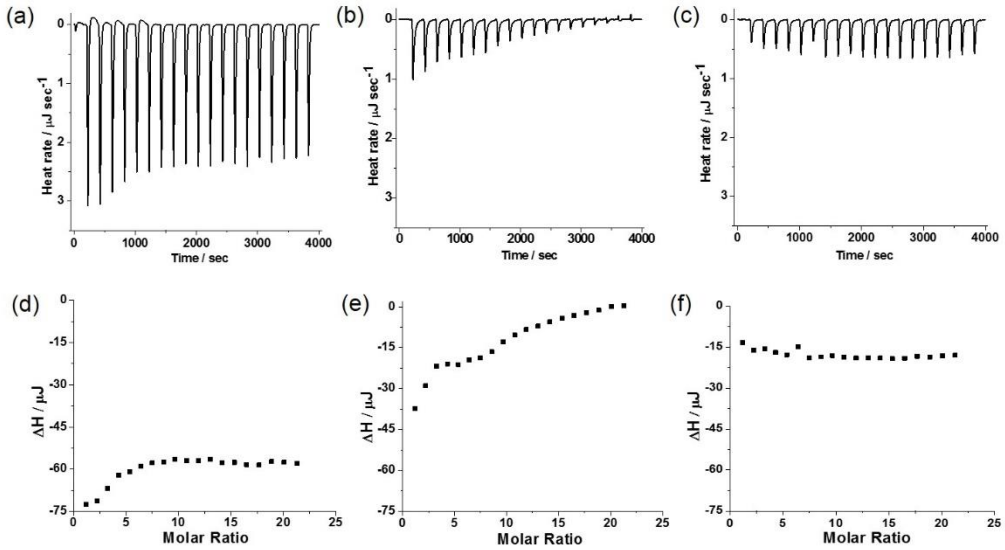

Figure S14. The top panel shows the ITC data for titration of **(a)** Ag^{I} vs DNA; **(b)** Ag^{I} vs **L1** and **(c) L1** vs mixture of DNA and Ag^{I}. The bottom panel (**d**, **e** and **f**) shows the plots of corresponding integrated heat data against molar ratio for same titrations. In all titrations, the former was taken in syringe and other in the cell. The total concentration of solutions taken in syringe and cell were 1 mM and 10 μM.

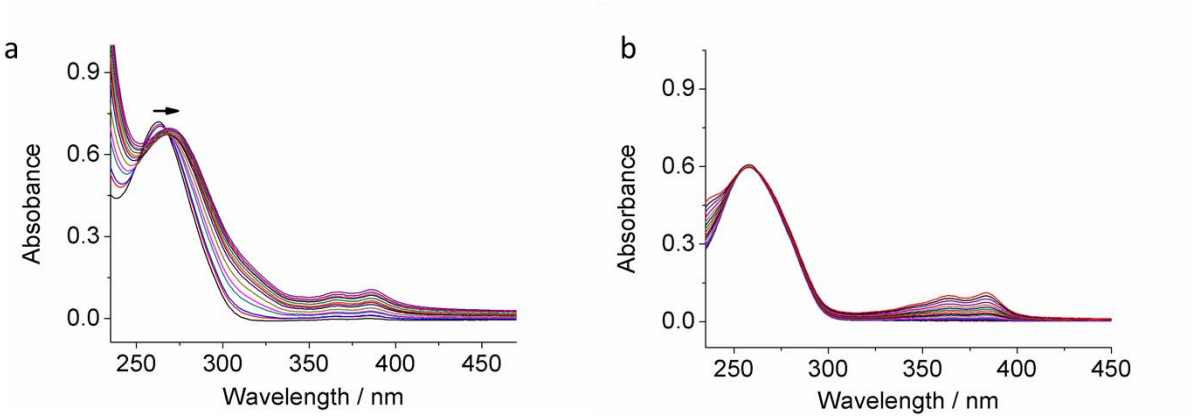

Figure S15. UV/vis spectra of a ctDNA solution (0.3 mM duplex, 1 mM $NaClO_4$, 5 mM MOPS, pH 6.8) titrated with a) **C2** and b) **L1** from 0 to 0.8 equiv. *r*-bound (ratio of concentration of binder/basepairs). When the ligand **L1** is titrated to the DNA, a minor decrease in the absorbance of the DNA is observed as **L1** intercalates into the base stack. In contrast, if **C2** is added to ctDNA, a shift in the absorbance maxima is detected (from 262 nm to 270 nm).

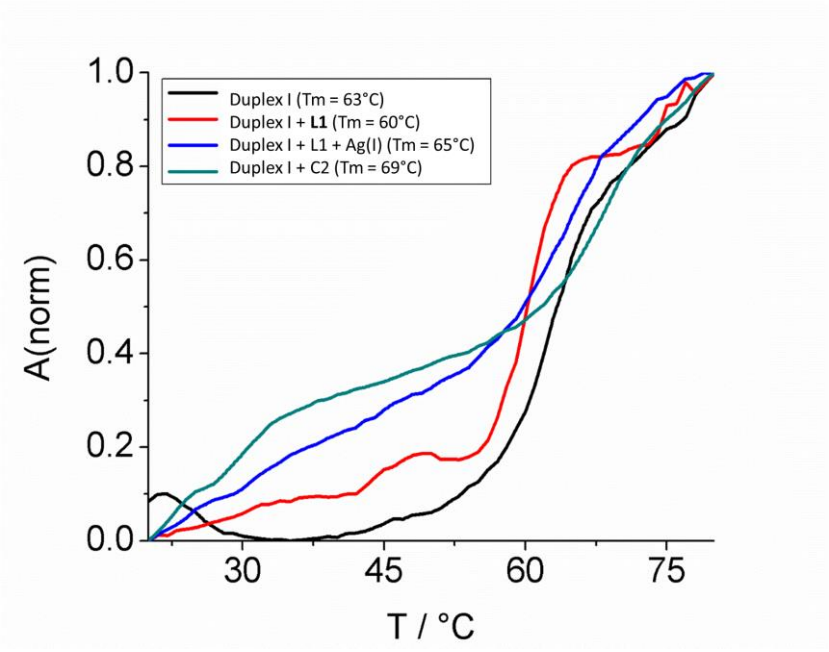

Figure S16. UV melting profiles of duplex **I** (black), duplex **I** with 10 **L1** molecules intercalated per duplex (red), a solution of duplex **I** with **L1** intercalated and subsequent addition of Ag^{I} (blue) and duplex **I** interacting with **C2**. Upon intercalation of **L1**, the melting point of the duplex decreases as expected for intercalation. When Ag^{I} is added, the melting point increases as the binding mode changes. This effect is even more pronounced when the premixed complex is added to duplex **I**.

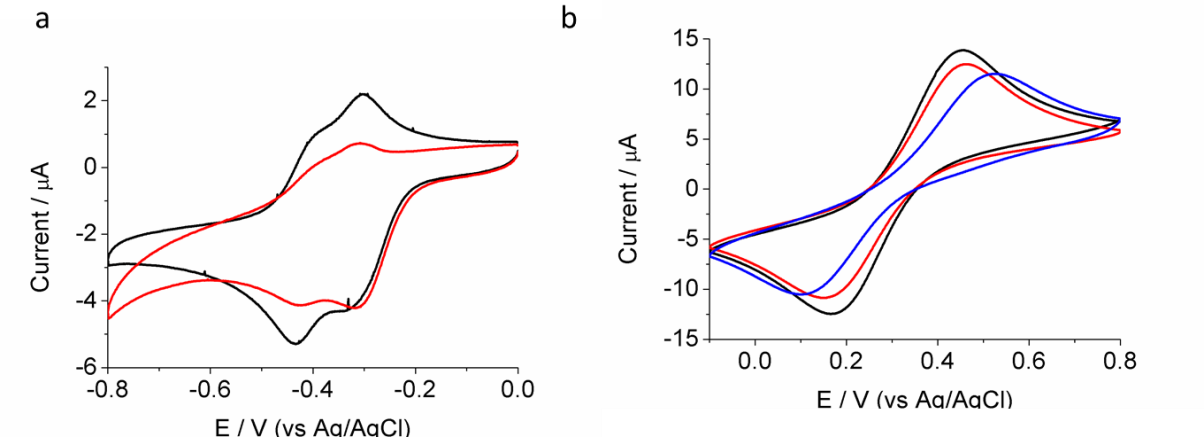

Figure S17. CV spectra of a) a solution of **L1** (black) and **C2** (red). 150 mM $NaClO_4$, 5 mM MOPS at pH 6.8 was added as the supporting electrolyte. Glassy carbon working electrode, Pt wire counter electrode and Ag/AgCl reference electrode were used. b) CV spectra of the $[Fe(CN)_6]^{3-/4-}$ redox probe in presence of immobilized DNA (black), DNA+**L1** (red) and DNA+**L1**+Ag^{I} (blue) on gold electrode. The experimental condition was same as stated before. $[Fe(CN)_6]^{3-/4-}$ redox probe was used as an external reference).

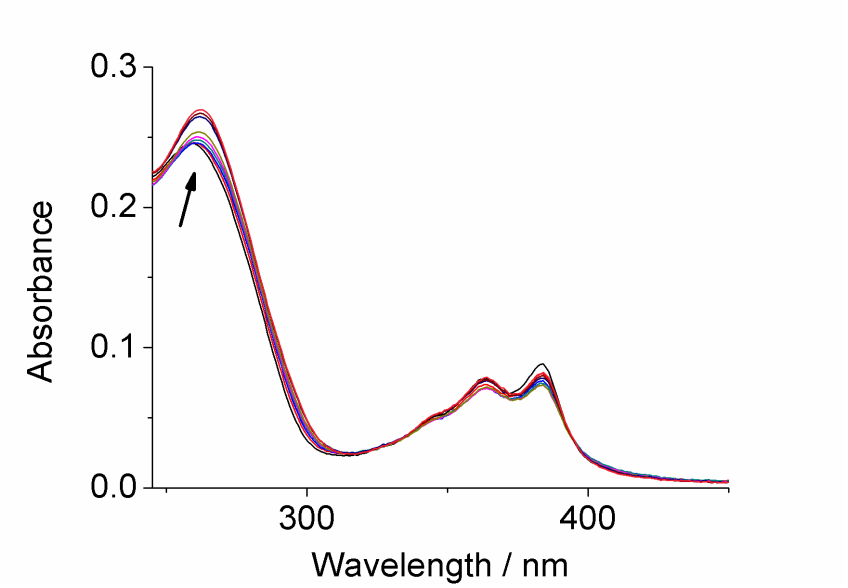

Figure S18. UV/vis spectra of duplex **I** in which 10 **L1** molecules are intercalated. Substoichiometric addition of $AgNO_3$ results in changes in the absorbance of the nucleic acid at around 260 nm as expected for the formation of complexes between Ag^I and **L1**. Experimental conditions: 1 µM duplex, 10 µM **L1**, 0 → 9 µM $AgNO_3$, 150 mM $NaClO_4$, 5 mM MOPS, pH 6.8).

Tables

Table S1. ITC derived thermodynamic parameters: binding constant (k_a), change in Gibbs free energy (ΔG), enthalpy change (ΔH) and entropy change (ΔS) for binding between the Ag^I, DNA and **L1** molecules at 298.15 K and pH 6.8. In all titrations, the former was taken in syringe and other in the cell.

System	k_a (M^{-1})	ΔG (kJ mol^{-1})	ΔH (kJ mol^{-1})	$T\Delta S$ (kJ mol^{-1})
Ag^I vs DNA	2.2×10^5	-30.5	4.70	35.2
Ag^I vs **L1**	6.0×10^5	-33.0	14.8	47.8
L1 vs DNA	-	-	-	-
Ag^I+**L1** vs DNA	2.3×10^5	-30.6	3.60	34.2
L1 vs DNA+Ag^I	-	-	-	-

Table S2. Crystal data and structure refinement for compound **L1**.

Empirical formula	$C_{28}H_{24}N_6O_9$
Formula weight	588.53
Temperature	150(2) K
Wavelength	1.54178 Å

Crystal system	Orthorhombic	
Space group	$P2_12_12_1$	
Unit cell dimensions	a = 9.2141(3) Å	α= 90°.
	b = 11.5864(4) Å	β= 90°.
	c = 25.4444(8) Å	γ = 90°.
Volume	2716.40(15) $Å^3$	
Z	4	
Density (calculated)	1.439 Mg/m^3	
Absorption coefficient	0.929 mm^{-1}	
F(000)	1224	
Crystal size	0.130 x 0.130 x 0.090 mm^3	
Theta range for data collection	3.474 to 67.336°.	
Index ranges	-10<=h<=10, -13<=k<=13, -30<=l<=30	
Reflections collected	55312	
Independent reflections	4804 [R(int) = 0.0481]	
Completeness to theta = 67.336°	99.0 %	
Absorption correction	Semi-empirical from equivalents	
Max. and min. transmission	0.7529 and 0.6867	
Refinement method	Full-matrix least-squares on F^2	
Data / restraints / parameters	4804 / 0 / 404	
Goodness-of-fit on F^2	1.069	
Final R indices [I>2sigma(I)]	R1 = 0.0283, wR2 = 0.0736	
R indices (all data)	R1 = 0.0286, wR2 = 0.0739	
Absolute structure parameter	0.07(3)	
Extinction coefficient	n/a	
Largest diff. peak and hole	0.191 and -0.172 $e.Å^{-3}$	

Table S3. Hydrogen bonds for compound **L1**.

D-H...A	d(D-H)	d(H...A)	d(D...A)	<(DHA)
N(4)-H(4N)...O(1W)	0.95(3)	1.87(4)	2.815(3)	172(3)

N(5)-H(5N)...N(3)#1	0.87(3)	2.10(3)	2.953(3)	167(3)
O(1W)-H(1WA)...N(6)	0.96(4)	1.87(4)	2.827(3)	173(4)
O(1W)-H(1WB)...O(5)#2	0.87(6)	2.41(6)	3.039(3)	129(5)

Symmetry transformations used to generate equivalent atoms:

#1 x,y-1,z #2 -x+1,y-1/2,-z+1/2

Table S4. Crystal data and structure refinement for the complex **C2**.

Empirical formula	$C_{85}H_{68}Ag_3BF_{10}N_{18}O_{27}Si$	
Formula weight	2326.08	
Temperature	151(2) K	
Wavelength	1.54178 Å	
Crystal system	Trigonal	
Space group	$P3_12_1$	
Unit cell dimensions	a = 26.1279(12) Å	α= 90°.
	b = 26.1279(12) Å	β= 90°.
	c = 26.9692(13) Å	γ = 120°.
Volume	15944.4(17) $Å^3$	
Z	6	
Density (calculated)	1.454 Mg/m^3	
Absorption coefficient	5.329 mm^{-1}	
F(000)	7020	
Crystal size	0.300 x 0.070 x 0.070 mm^3	
Theta range for data collection	1.952 to 67.488°.	
Index ranges	-31<=h<=31, -31<=k<=31, -32<=l<=31	
Reflections collected	310552	
Independent reflections	18655 [R(int) = 0.1058]	
Completeness to theta = 67.488°	98.4 %	
Absorption correction	Semi-empirical from equivalents	
Max. and min. transmission	0.7395 and 0.4561	
Refinement method	Full-matrix least-squares on F^2	
Data / restraints / parameters	18655 / 12 / 1302	
Goodness-of-fit on F^2	1.063	
Final R indices [I>2sigma(I)]	R1 = 0.0501, wR2 = 0.1344	
R indices (all data)	R1 = 0.0599, wR2 = 0.1415	

Absolute structure parameter	0.010(2)
Extinction coefficient	n/a
Largest diff. peak and hole	1.265 and -2.168 e.Å^{-3}

Table S5. Selected Bond lengths [Å] and angles [°] for the complex **C2**.

Ag(1A)-N(4A)#1	2.095(5)
Ag(1A)-N(4A)	2.095(5)
Ag(2A)-N(7A)	2.047(9)
Ag(2A)-N(6A)	2.068(9)
Ag(1B)-N(4B)	2.093(6)
Ag(1B)-N(4B)#2	2.093(6)
Ag(2B)-N(7B)	2.091(7)
Ag(2B)-N(6B)	2.096(6)
Si(1)-F(2)	1.646(8)
Si(1)-F(1)	1.655(8)
Si(1)-F(6)	1.672(7)
Si(1)-F(3)	1.674(9)
Si(1)-F(5)	1.674(6)
Si(1)-F(4)	1.676(7)
B(1)-F(7)#1	1.370(10)
B(1)-F(7)	1.370(10)
B(1)-F(8)	1.389(10)
B(1)-F(8)#1	1.389(10)
B(2)-F(10)#2	1.374(10)
B(2)-F(10)	1.374(10)
B(2)-F(9)#2	1.376(11)
B(2)-F(9)	1.376(11)
N(4A)#1-Ag(1A)-N(4A)	176.9(3)
N(7A)-Ag(2A)-N(6A)	168.4(4)
N(4B)-Ag(1B)-N(4B)#2	176.5(4)
N(7B)-Ag(2B)-N(6B)	170.4(3)
C(28B)-N(6B)-Ag(2B)	124.6(6)
C(26B)-N(6B)-Ag(2B)	127.0(5)
C(29B)-N(7B)-Ag(2B)	128.6(6)

C(31B)-N(7B)-Ag(2B)	124.4(6)
F(2)-Si(1)-F(1)	89.7(6)
F(2)-Si(1)-F(6)	88.2(5)
F(1)-Si(1)-F(6)	177.7(5)
F(2)-Si(1)-F(3)	91.3(6)
F(1)-Si(1)-F(3)	89.0(5)
F(6)-Si(1)-F(3)	90.0(4)
F(2)-Si(1)-F(5)	178.9(5)
F(1)-Si(1)-F(5)	91.4(4)
F(6)-Si(1)-F(5)	90.7(4)
F(3)-Si(1)-F(5)	88.9(4)
F(2)-Si(1)-F(4)	89.6(5)
F(1)-Si(1)-F(4)	92.6(5)
F(6)-Si(1)-F(4)	88.4(3)
F(3)-Si(1)-F(4)	178.2(5)
F(5)-Si(1)-F(4)	90.2(3)
F(7)#1-B(1)-F(7)	109.1(12)
F(7)#1-B(1)-F(8)	109.0(5)
F(7)-B(1)-F(8)	110.6(4)
F(7)#1-B(1)-F(8)#1	110.6(4)
F(7)-B(1)-F(8)#1	109.0(5)
F(8)-B(1)-F(8)#1	108.7(11)
F(10)#2-B(2)-F(10)	110.4(12)
F(10)#2-B(2)-F(9)#2	109.2(4)
F(10)-B(2)-F(9)#2	109.8(4)
F(10)#2-B(2)-F(9)	109.8(4)
F(10)-B(2)-F(9)	109.2(4)
F(9)#2-B(2)-F(9)	108.4(13)

Symmetry transformations used to generate equivalent atoms:

#1 x-y,-y,-z+5/3 #2 -x+2,-x+y+1,-z+4/3

Table S6. Values of the equivalent circuit elements shown in Scheme S2 obtained from EIS measurements. R_S was kept constant at 0.04(2) kΩ.

	C_M / nF	R_{CT}/kΩ	R_X/kΩ	CPE /μF	n	ΔR_{CT}/%
Duplex	*6 ± 0.3*	*7 ± 3*	*0.135 ± 0.001*	*0.7 ± 0.1*	*0.94 ± 0.02*	

*Duplex + **L1***	*6 ± 0.7*	*10 ± 5*	*0.136 ± 0.007*	*0.6 ± 0.2*	*0.94 ± 0.02*	*34 ± 17*
*Duplex + **L1** + Ag(I)*	*7 ± 0.8*	*17 ± 8*	*0.130 ± 0.008*	*0.6 ± 0.2*	*0.95 ± 0.01*	*71 ± 7*
Duplex	*6 ± 0.7*	*7 ± 1*	*0.146 ± 0.07*	*0.6 ± 0.1*	*0.94 ± 0.01*	
*Duplex + **C2***	*6 ± 0.8*	*20 ± 2*	*0.135 ± 0.07*	*0.6 ± 0.1*	*0.94 ± 0.01*	200 ± *10*

References

[1] a) J. C. Léon, Z. She, A. Kamal, M. H. Shamsi, J. Müller, H. B. Kraatz, *Angew. Chem.* **2017**, *129*, 6194-6198; *Angew. Chem. Int. Ed.* **2017**, *56*, 6098-6102. b) K. Schweizer, J. C. Léon, B. J. Ravoo, J. Müller, *J. Inorg. Biochem.* **2016**, *160*, 256-263. c) K. Petrovec, B. J. Ravoo, J. Müller, *Chemical Communications* **2012**, *48*, 11844-11846.

[2] H. Gong, X. H. Li, *Analyst* **2011**, *136*, 2242-2246.

[3] H. Gong, T. Y. Zhong, L. Gao, X. H. Li, L. J. Bi, H. B. Kraatz, *Analytical Chemistry* **2009**, *81*, 8639-8643.

[4] a) M. G. Freire, C. M. S. S. Neves, I. M. Marrucho, J. A. P. Coutinho, A. M. Fernandes, *J. Phys. Chem. A* **2010**, *114*, 3744-3749; b) D. M. Knotter, *J. Am. Chem. Soc.* **2000**, *122*, 4345-4351.

[5] I. S. Tidmarsh, B. F. Taylor, M. J. Hardie, L. Russo,c W. Clegg, M. D. Ward, *New J. Chem.* **2009**, *33*, 366–375.